UCSF
UC San Francisco Previously Published Works

Title

Genetic predisposition to altered blood cell homeostasis is associated with glioma risk and survival

Permalink

https://escholarship.org/uc/item/7wj446k5

Journal

Nature Communications, 16(1)

ISSN

2041-1723

Authors

Kachuri, Linda

Guerra, Geno A

Nakase, Taishi

et al.

Publication Date
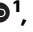
2025

DOI

10.1038/s41467-025-55919-6

Peer reviewed

Genetic predisposition to altered blood cell homeostasis is associated with glioma risk and survival

Linda Kachuri [1,2] ✉, Geno A. Guerra[3,4], Taishi Nakase [1], George A. Wendt[3], Helen M. Hansen [3], Annette M. Molinaro [3,4], Paige Bracci[4], Lucie McCoy [3], Terri Rice[3], John K. Wiencke [3,5], Jeanette E. Eckel-Passow[6], Robert B. Jenkins[7], Margaret Wrensch[3] & Stephen S. Francis[3,4,5] ✉

Glioma is a highly fatal and heterogeneous brain tumor with few known risk factors. Our study examines genetically predicted variability in blood cell indices in relation to glioma risk and survival in 3418 cases and 8156 controls. We find that increased platelet to lymphocyte ratio (PLR) confers an increased risk of glioma (odds ratio (OR) = 1.25, p = 0.005), especially tumors with isocitrate dehydrogenase (IDH) mutations (OR = 1.38, p = 0.007) and IDH_{mut} 1p/19q intact ($IDH_{mut-intact}$ OR = 1.53, p = 0.004) tumors. Genetically inferred increased counts of lymphocytes ($IDH_{mut-intact}$ OR = 0.70, p = 0.004) and neutrophils (IDH_{mut} OR = 0.69, p = 0.019; $IDH_{mut-intact}$ OR = 0.60, p = 0.009) show inverse associations with risk, which may reflect enhanced immune-surveillance. Considering survival, we observe higher mortality risk in patients with IDH_{mut} 1p/19q with genetically predicted increased counts of lymphocytes (hazard ratio (HR) = 1.65, 95% CI: 1.24–2.20), neutrophils (HR = 1.49, 1.13–1.97), and eosinophils (HR = 1.59, 1.18–2.14). Polygenic scores for blood cell traits are also differentially associated with 17 tumor immune microenvironment features in a subtype-specific manner, including signatures related to interferon signaling, PD-1 expression, and T-cell/Cytotoxic responses. Our findings highlight immune-mediated susceptibility mechanisms with potential disease management implications.

Glioma is the most common malignant central nervous system tumor in the United States and globally[1,2]. Despite being a relatively rare primary cancer, gliomas make an outsize contribution to cancer mortality due to limited advances in treatment. Identification of molecular subtypes, which have been incorporated into the World Health Organization (WHO) brain tumor classification scheme since 2016, has helped delineate gliomas with distinct clinical presentation and survival trajectories beyond traditional histopathologic categories. Two major molecular features used to classify gliomas are mutations in *IDH1* (isocitrate dehydrogenase 1) or *IDH2* genes, collectively referred to as IDH mutations, and chromosome 1p and 19q co-deletion status[3,4]. Patients with IDH-mutant gliomas have a more favorable prognosis, but these tumors tend to progress, recur as higher grades, and become resistant to therapy. IDH wildtype tumors are the most aggressive, with

[1]Department of Epidemiology & Population Health, Stanford University School of Medicine, Stanford, CA, USA. [2]Stanford Cancer Institute, Stanford University School of Medicine, Stanford, CA, USA. [3]Department of Neurological Surgery, University of California San Francisco, San Francisco, CA, USA. [4]Department of Epidemiology & Biostatistics, University of California San Francisco, San Francisco, CA, USA. [5]Weill Institute for Neurosciences, University of California San Francisco, San Francisco, CA, USA. [6]Division of Biomedical Statistics and Informatics, Mayo Clinic, Rochester, MN, USA. [7]Department of Laboratory Medicine and Pathology, Mayo Clinic, Rochester, MN, USA. ✉e-mail: lkachuri@stanford.edu; stephen.francis@ucsf.edu

a median survival of only 1.2 years, compared to 17.5 years for patients with IDH mutation and 1p/19q co-deletion[4,5].

There are few non-genetic risk factors for glioma and even less is known about differences in putative risk factors across molecular subtypes. Exposure to ionizing radiation is the only established causal factor, although it accounts for a low proportion of glioma cases at the population level[4]. An accumulation of findings from observational studies makes a compelling case for an immune component in glioma etiology. History of infection with varicella zoster virus (VZV), a neurotropic α-herpesvirus that causes chickenpox and shingles[6,7], and the presence of IgG antibodies to VZV[7] have been inversely associated with glioma risk. This has recently extended to prognosis, where stronger VZV reactivity was associated with improved survival[8]. History of allergies or other atopic conditions (hay fever, eczema, and asthma)[9–12] and increased IgE levels[13,14] have been associated with a decreased risk of glioma in multiple observational studies. However, an analysis using genetic variants associated with atopic conditions and IgE levels did not support these findings and detected only inconsistent protective effects for atopic dermatitis[15]. Other genetic association studies have uncovered protective effects of stronger immune reactivity to viral infection[16] and an inverse relationship between genetic susceptibility to glioma and autoimmune conditions[17].

The mechanisms underlying these associations with immune function remain elusive. One candidate hypothesis for the observed protective effects relates to heightened immune activation and improved immunosurveillance that translates into enhanced tumor clearance[4,10,13]. Commonly measured hematologic indices, such as counts of white blood cells and platelets, reflect systemic immune and inflammatory responses and are frequently dysregulated in cancer patients. Immune dysregulation is well documented in glioma patients[18–20]. Low proportions of CD4 T-cells have been linked to diminished survival[5,21]. While these observations may be relevant for prognostic stratification, the potential etiologic role of alterations in immune cells profiles is confounded by effects of dexamethasone treatment and systemic changes caused by the disease process[20].

In this study, we leverage a large collection of glioma cases with genome-wide genetic data and information on molecular subtypes to examine how genetic predisposition to increased counts of leukocytes and platelets relate to glioma risk and survival. Genome-wide association studies (GWAS) have demonstrated overlap between genetic loci involved in the regulation of blood cell traits and cancer susceptibility[22–24]. Furthermore, host immune responses to infection and cancer share important, evolutionarily conserved, pathways, many of which are dependent on platelet- and leukocyte-driven processes. By relying on germline determinants of constitutive variation in blood cell counts, Mendelian randomization (MR) provides associations that are not affected by reverse causation, a major limitation of observational studies due to alterations in immune cell frequencies caused by tumorigenesis and treatment. In addition to investigating glioma susceptibility, we also comprehensively characterize the role of genetically predicted immune cell frequencies with overall glioma survival.

Results
Genetically inferred blood cell profiles and glioma risk
Summary statistics were available from a GWAS meta-analysis of 3418 glioma cases with available molecular profiling and 8156 controls. The majority of cases ($n = 1479$) had IDH wildtype (IDH_{wt}) tumors. A total of 1074 cases harbored somatic *IDH1*/*IDH2* mutations (IDH_{mut}), of which 396 were also 1p/19q co-deleted ($IDH_{mut-codel}$) while 622 had 1p/19q intact ($IDH_{mut-intact}$).

For most blood cell traits, Cochran's Q ($P_Q < 0.05$) and the PRESSO Global test ($P_{Global} < 0.05$) detected heterogeneity among the causal effects implied by individual instruments (Supplementary Table 1). In such cases, the inverse variance weighted multiplicative random-effects (IVW-MRE) estimator replaced the maximum likelihood (ML) as

the default estimate against which other MR estimators were compared. Associations that exhibited consistency across MR-PRESSO[25], MR-RAPS[26,27], and weighted median (WM)[28] were considered reliable.

Analysis of glioma overall identified a signal for platelet to lymphocyte ratio (PLR) (Fig. 1; Supplementary Table 2), suggesting that genetic predisposition to an increase in the relative abundance of platelets to lymphocytes confers an increased glioma risk ($OR_{ML} = 1.25$, 95% CI: 1.10–1.43, $p = 9.1 \times 10^{-4}$). These results persisted in sensitivity analyses ($OR_{IVW-MRE} = 1.25$, $p = 4.9 \times 10^{-3}$; $OR_{PRESSO} = 1.21$, $p = 8.8 \times 10^{-3}$; $OR_{RAPS} = 1.22$, $p = 0.011$). There was evidence of directional horizontal pleiotropy (Egger $\beta_0 \neq 0$, $p < 0.05$) for eosinophils, lymphocytes, monocytes, and platelets (Supplementary Table 1). Accounting for this using MR Egger detected an inverse association with risk of glioma for increasing eosinophil counts ($OR_{Egger} = 0.67$, 0.46–0.99, $p = 0.044$). Regression dilution bias due to measurement error[29] did not appear to affect MR Egger analyses, as indicated by $I^2_{GX} > 0.98$ for all phenotypes (Supplementary Table 1).

Associations with genetically predicted blood cell profiles differed across major molecular subtypes of glioma. Statistically significant associations (false discovery rate (FDR) < 0.05) were primarily observed for IDH_{mut} and $IDH_{mut-intact}$ tumors (Fig. 2; Supplementary Table 3), but not with IDH_{wt} tumors, despite the larger sample size for this subtype (Fig. 3; Supplementary Table 4). An increase in neutrophil counts was inversely associated with the risk of IDH_{mut} tumors ($OR_{IVW-MRE} = 0.69$, 0.50–0.94, $p = 0.019$) and this was more pronounced for the $IDH_{mut-intact}$ ($OR_{IVW-MRE} = 0.60$, 0.41–0.88, $p = 9.1 \times 10^{-3}$) subtype (Fig. 2; Supplementary Table 3). Association with neutrophils remained consistent across MR methods for IDH_{mut} ($OR_{PRESSO} = 0.67$, $p = 0.011$; $OR_{RAPS} = 0.68$, $p = 0.024$; $OR_{WM} = 0.67$, $p = 0.011$) and $IDH_{mut-intact}$ ($OR_{PRESSO} = 0.60$, $p = 9.1 \times 10^{-3}$; $OR_{RAPS} = 0.61$, $p = 0.017$; $OR_{WM} = 0.60$, $p = 9.6 \times 10^{-3}$). In $IDH_{mut-codel}$ tumors the effect of neutrophil counts was attenuated and not statistically significant ($OR_{IVW-MRE} = 0.80$, $p = 0.31$).

We also detected an inverse association with higher lymphocyte counts and risk of $IDH_{mut-intact}$ glioma ($OR_{IVW-MRE} = 0.70$, 0.55–0.89, $p = 3.8 \times 10^{-3}$). This relationship was supported by most MR models ($OR_{PRESSO} = 0.70$; $OR_{RAPS} = 0.67$), except for the weighted median ($OR_{WM} = 1.00$, $p = 0.98$). Increased lymphocyte counts were not associated with a lower risk of IDH_{mut} or $IDH_{mut-codel}$ gliomas.

The PLR association detected for glioma overall was also observed for IDH_{mut} glioma ($OR_{IVW-MRE} = 1.38$, $p = 7.2 \times 10^{-3}$) and $IDH_{mut-intact}$ tumors ($OR_{IVW-MRE} = 1.53$, $p = 3.7 \times 10^{-3}$), but not $IDH_{mut-codel}$ ($OR_{IVW-MRE} = 1.15$, $p = 0.43$) (Supplementary Table 3). PLR appeared to be associated with risk of IDH_{wt} tumors ($OR_{ML} = 1.23$, $p = 0.017$), but the direction of this estimate became reversed and not statistically significant after correcting for horizontal pleiotropy ($OR_{Egger} = 0.83$, $p = 0.42$; Egger $\beta_0 = 0.014$, $p = 0.059$). In addition to MR-PRESSO, we also filtered potentially invalid instruments based on outlier detection implemented by MR Radial[30] and re-fit MR IVW models on the remaining variants (Supplementary Table 5). These sensitivity analyses confirmed the subtype-specific associations observed for lymphocytes and $IDH_{mut-intact}$ glioma (OR = 0.69, $p = 4.5 \times 10^{-4}$), neutrophils (IDH_{mut}: OR = 0.65, $p = 1.4 \times 10^{-3}$; $IDH_{mut-intact}$: OR = 0.61, $p = 5.2 \times 10^{-3}$), and PLR (glioma: OR = 1.27, $p = 2.2 \times 10^{-4}$; IDH_{mut}: OR = 1.45, $p = 3.1 \times 10^{-4}$; $IDH_{mut-intact}$: OR = 1.53, $p = 8.1 \times 10^{-4}$). As a final sensitivity analysis, MR Steiger[31] was applied to test whether the assumption that the exposure causes the outcome is valid. For all associated exposure-outcome pairs, statistically significant Steiger p-values confirmed the correct orientation of the observed relationship: PLR (glioma $p = 3.9 \times 10^{-72}$; IDH_{mut} $p = 8.7 \times 10^{-43}$; $IDH_{mut-intact}$ $p = 4.0 \times 10^{-41}$), neutrophils (IDH_{mut} $p = 3.4 \times 10^{-17}$; $IDH_{mut-intact}$ $p = 3.9 \times 10^{-16}$), and lymphocytes (IDH_{mut} $p = 2.1 \times 10^{-41}$; $IDH_{mut-intact}$ $p = 4.1 \times 10^{-43}$).

Multivariable MR analyses suggested that only genetically predicted lymphocytes were independently associated with $IDH_{mut-intact}$

glioma risk ($OR_{MV\text{-}IVW} = 0.70$, 0.48–1.00, $p = 0.051$) (Supplementary Table 6). Applying MV-LASSO to a set of independent instruments across lymphocytes, neutrophils, platelets, and PLR resulted in the removal of platelets and shrunk the effect sizes of the remaining three traits ($OR_{MV\text{-}LASSO} = 1.16$ for PLR; $OR_{MV\text{-}LASSO} = 0.89$ for lymphocytes; $OR_{MV\text{-}LASSO} = 0.90$ for neutrophils). Only PLR ($OR_{MV\text{-}LASSO} = 1.11$) and neutrophils ($OR_{MV\text{-}LASSO} = 0.86$) were retained for IDH_{mut}.

Colocalization of glioma risk loci with blood cell traits

Among genetic instruments for blood cell traits, we identified 8 variants that reached genome-wide significance for at least one glioma phenotype and focused our fine-mapping and colocalization analyses on these loci (Supplementary Table 7). If SuSiE[32,33] identified multiple independent credible sets for either trait, we looked for evidence of colocalization with at least one fine-mapped signal (Supplementary Table 8). We also performed multi-trait colocalization using HyprColoc to identify a set of traits that share a single causal signal. In the 2q37.3 (*D2HGDH*) region the susceptibility signal for $IDH_{mut\text{-}intact}$ glioma was

attributed to a single variant (rs78147778, $p = 7.7 \times 10^{-11}$), which colocalized with the lead signal for eosinophil counts at rs34290285 ($p = 3.9 \times 10^{-37}$; $PP_{H4} = 0.939$), but not with the weaker secondary signal at rs79245503 (Fig. 4; Source Data File). The only lead signal for IDH_{mut} in 8q24.21 (rs55705857, $p = 3.0 \times 10^{-55}$) was distinct ($PP_{H4} = 0$) from all fine-mapped variants for LMR, monocytes, and platelets. Multi-trait colocalization identified a shared causal signal for LMR and monocytes ($PP_{H4} = 0.972$).

Several glioma risk variants and blood cell instruments were found in regions that harbored important genes for telomere maintenance: telomerase reverse transcriptase (*TERT*) in 5p15.33 and regulator of telomere elongation helicase 1 (*RTEL1*) in 20q13.33. Since telomere length is an established risk factor for glioma and the putative causal mechanism in these regions, it was incorporated into the colocalization analyses[34,35]. Fine-mapping in 5p15.33 detected the same causal variant for glioma overall (rs7726159, $p = 3.0 \times 10^{-24}$) and IDH_{wt} (rs7726159, $p = 3.0 \times 10^{-25}$; Supplementary Fig. 2), which colocalized with the lead variant for PLR (rs7705526; $PP_{H4} = 0.984$ and
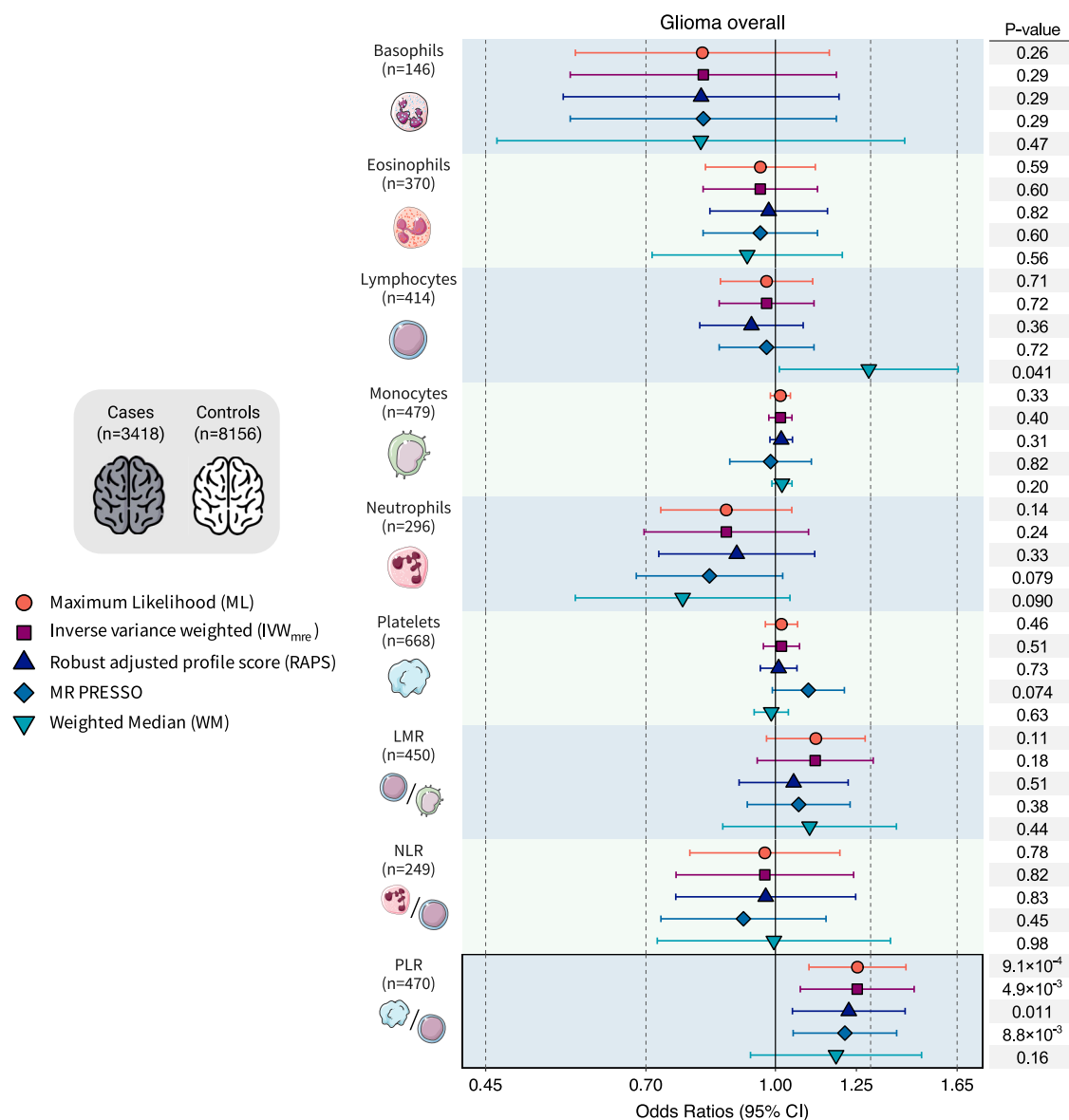

Fig. 1 | Mendelian randomization results for glioma overall. Visualization of odds ratios (OR) and 95% confidence intervals (CI) for the effect of increasing blood cell counts or blood cell ratios on the risk of glioma overall (3184 cases, 8156 controls). For each blood cell phenotype, association results, including two-sided *p*-values, are reported for five Mendelian randomization estimation methods.
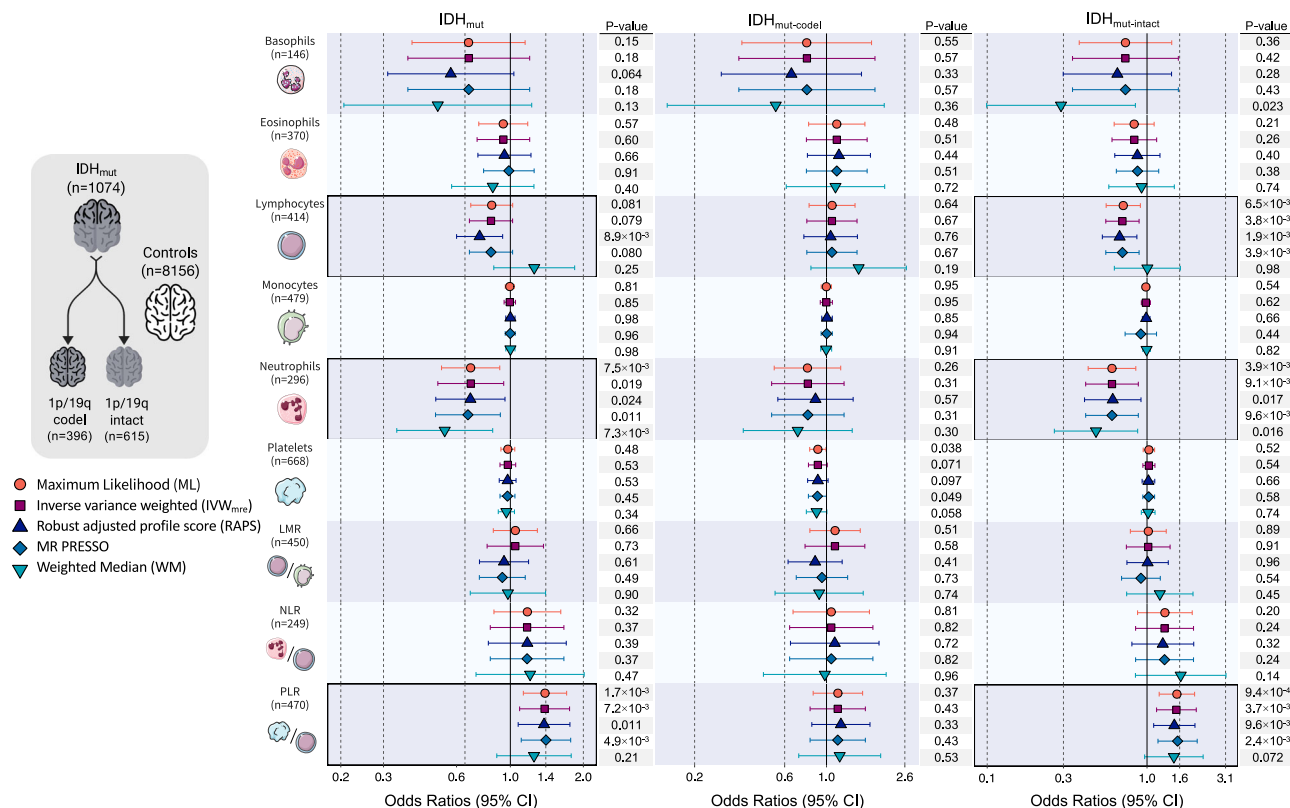
Fig. 2 | Mendelian randomization results for IDH mutated (IDH$_{mut}$) glioma. Visualization of odds ratios (OR) and 95% confidence intervals (CI) for the effect of increasing blood cell counts or blood cell ratios on the risk of IDH$_{mut}$ glioma and further stratified by the presence of 1p/19q co-deletion. For each blood cell phenotype and Mendelian randomization estimation method, two-sided p-values are reported.

PP$_{H4}$ = 0.996, respectively), but not with NLR (rs2853677, PP$_{H4}$ = 0). For phenotypes with multiple independent signals, glioma, and IDH$_{wt}$ colocalized at PP$_{H4}$ > 0.98 with one of several lead variants for platelets (rs7705526), neutrophils (rs7725218), and telomere length (rs7705526). Lastly, in 20q13.33 there was evidence of colocalization for IDH$_{wt}$ (rs6062302, $p = 6.5 \times 10^{-18}$; with platelets (rs4809319, $p = 1.1 \times 10^{-9}$; PP$_{H4}$ = 0.947), but not with any of the five signals for telomere length (PP$_{H4}$ = 0; Supplementary Fig. 2; Supplementary Table 8).

Prognostic associations for genetic predictors of blood cell traits

We explored whether genetic instruments for blood cell trait variation predict survival in glioma patients (see Supplementary Table 9 for baseline characteristics). Each blood cell trait polygenic score (PGS) was comprised of the same variants and weights as the instruments used in the MR analysis of glioma risk. Survival analyses were conducted separately in each study (Supplementary Table 10) and meta-analyzed across the three case-series (Fig. 5; Supplementary Table 11). The meta-analysis identified four statistically significant (FDR < 0.05) associations, all of which were restricted to the IDH$_{mut-codel}$ subtype with 370 cases and 78 deaths (Supplementary Table 11). We observed an increased risk of mortality per SD increase in the PGS for basophils (HR = 1.39, 95% CI: 1.06–1.83, $p = 0.018$), eosinophils (HR = 1.58, 1.17–2.13, $p = 2.6 \times 10^{-3}$), lymphocytes (HR = 1.68, 1.25–2.26, $p = 5.1 \times 10^{-4}$), and neutrophils (HR = 1.44, 1.08–1.92, $p = 0.013$). There was evidence of heterogeneity for the neutrophil association (Cochran's Q p-value = 0.024, I^2 = 0.80). Although the study-specific estimates had concordant directions of effect, the magnitude of the association was much larger in TCGA cases (HR = 4.82, 1.63–14.29, $p = 4.5 \times 10^{-3}$) than in the combined UCSF AGS and Mayo Clinic patient population (HR = 1.37, 1.03–1.83, $p = 0.033$).

Treatment information was only available from UCSF and Mayo Clinic, with variable levels of missingness. PGS associations adjusted for grade, chemotherapy, and radiation were directionally concordant with minimally adjusted results, although most HR estimates were attenuated due to reduced sample size (Supplementary Table 12). In 160 IDH$_{mut-codel}$ patients with available clinical data, the lymphocyte PGS remained associated with increased mortality (HR = 1.67, 1.18–2.38, $p = 3.9 \times 10^{-3}$). We also observed an inverse association with mortality for the NLR PGS (HR = 0.59, 0.42–0.81, $p = 1.3 \times 10^{-3}$).

Prior to evaluating associations with survival using Mendelian randomization, we tested for the presence of index event bias. Based on a set of pruned independent variants, the regression of survival log(HR) on incidence log(OR), with SIMEX adjustment for regression dilution, yielded a coefficient of −0.084 (95% CI: −0.101 to −0.072) for glioma and −0.137 (95% CI: −0.325 to −0.087) for IDH$_{mut}$. This implies there are common causes of incidence and prognosis, the net effect of which produces modestly biased effects on survival for blood cell traits that are also associated with risk.

We present MR results based on unadjusted and bias-corrected instrument effects on survival, although the correction did not have an appreciable impact (Supplementary Table 13). MR findings were generally concordant with PGS analyses, indicating an increased risk of death conferred by genetic predisposition to elevated counts of basophils (HR$_{IVW-MRE}$ = 13.18, p = 0.018), eosinophils (HR$_{IVW-MRE}$ = 3.87, $p = 1.9 \times 10^{-3}$), lymphocytes (HR$_{IVW-MRE}$ = 4.36, $p = 3.2 \times 10^{-5}$), and neutrophils (HR$_{IVW-MRE}$ = 4.51, $p = 3.2 \times 10^{-3}$). MR estimates were substantially larger than in PGS analyses, but they also had extremely wide 95% confidence intervals due to the large variance of SNP-specific effect sizes. Therefore, while we establish the direction of the putative causal effect on glioma mortality, it is difficult to accurately infer its magnitude.
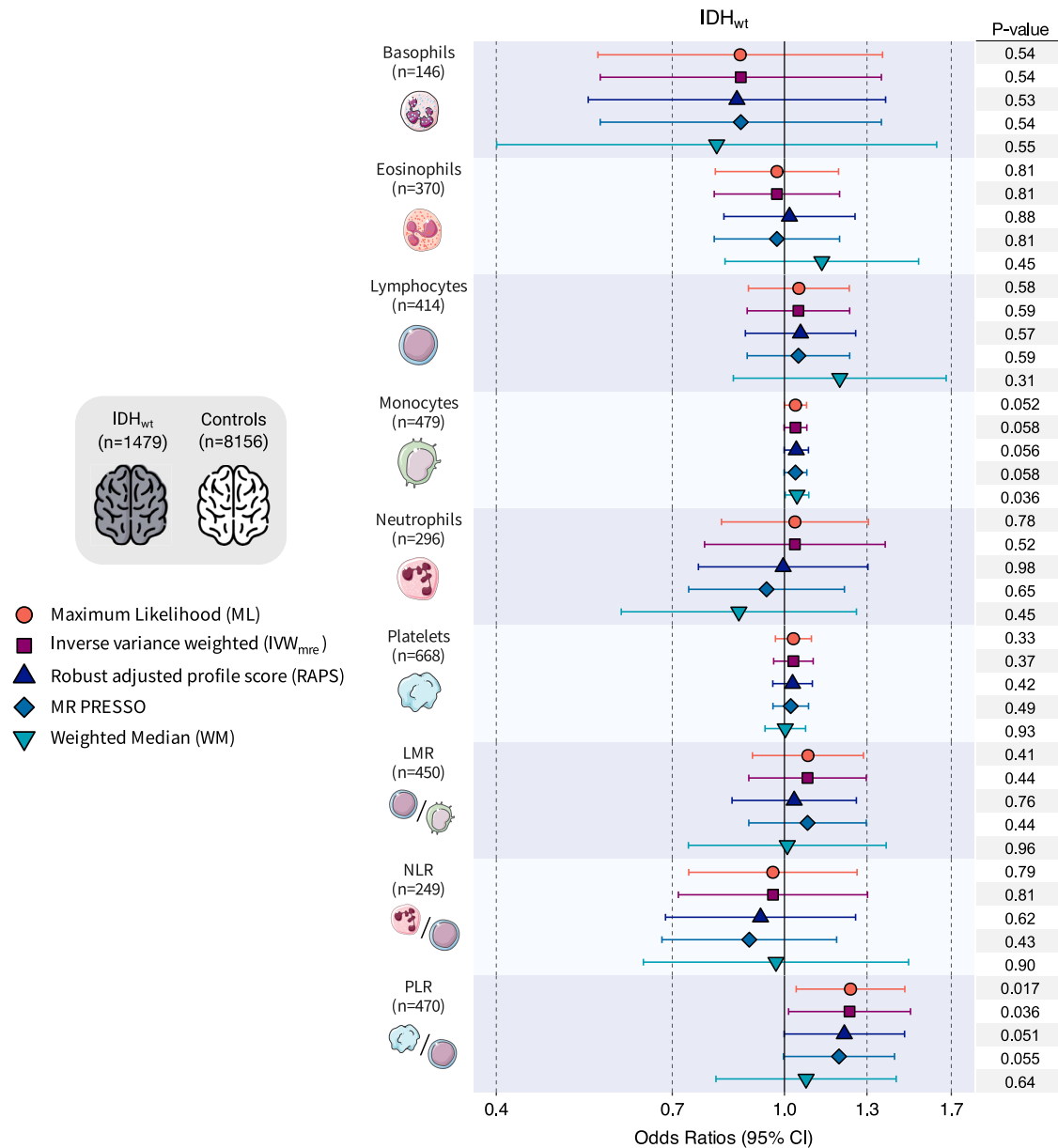
Fig. 3 | Mendelian randomization results for IDH wildtype (IDH$_{wt}$) glioma. Visualization of Mendelian randomization odds ratios (OR) and 95% confidence intervals (CI) for the effect of increasing blood cell counts or blood cell ratios on the risk of IDH$_{wt}$ glioma overall. For each blood cell phenotype and Mendelian randomization estimation method, two-sided *p*-values are reported.

Genetic associations with glioma tumor immune microenvironment features

To gain insight into potential tumorigenic mechanisms underlying the associations observed for blood cell traits, we examined their PGS associations with features of the heritable tumor immune microenvironment (TIME). Using data on 28 heritable TIME features identified by Sayaman et al.[36] in TCGA, we conducted PGS analyses stratified by IDH mutation status (Fig. 6; Supplementary Fig. 3; Supplementary Data 1). No associations reached FDR < 0.05 for IDH$_{mut}$, but the neutrophil PGS was suggestive (FDR < 0.10) associated with several signatures in the T-cell/Cytotoxic module, including enrichment scores for neutrophils, effector memory T-cells (T$_{EM}$), and T-helper 17 cells (Th17). Among IDH$_{wt}$ tumors the lymphocyte PGS was positively associated with CD8 + T-cell enrichment ($p = 1.3 \times 10^{-3}$, FDR = 0.036).

There was significant effect size heterogeneity ($P_{het} < 0.05$) in the PGS associations for 17 traits when comparing estimates in IDH$_{mut}$ and IDH$_{wt}$ groups (Fig. 5). Most of the differential PGS effects were observed for TIME traits in IFN response and T-cell/Cytotoxic modules. Genetic scores for PLR and lymphocytes had the largest number of heterogeneous TIME associations (11 traits), followed by neutrophils and basophils (3 traits). The largest differences in genetic associations between IDH$_{mut}$ and IDH$_{wt}$ tumors were observed for activated dendritic cells ($P_{het} = 8.9 \times 10^{-4}$), CD8 T-cells ($P_{het} = 8.2 \times 10^{-4}$), T-helper cells ($P_{het} = 4.3 \times 10^{-9}$), multiple IFN signatures, and gene-based signatures G SIGLEC9 ($P_{het} = 0.012$), MHC II ($P_{het} = 0.019$), and PD-1 ($P_{het} = 0.049$).

Discussion

Blood cell counts are routinely measured in clinical settings to assess overall health, including systemic response to infection, inflammation, and allergic reactions. Markers of immune function, including blood cell proportions, have been associated with glioma survival[5,21] and are used to monitor adverse effects of chemotherapy and radiation. However, the etiologic role of blood cell profiles has not been comprehensively investigated, partly because they are influenced by
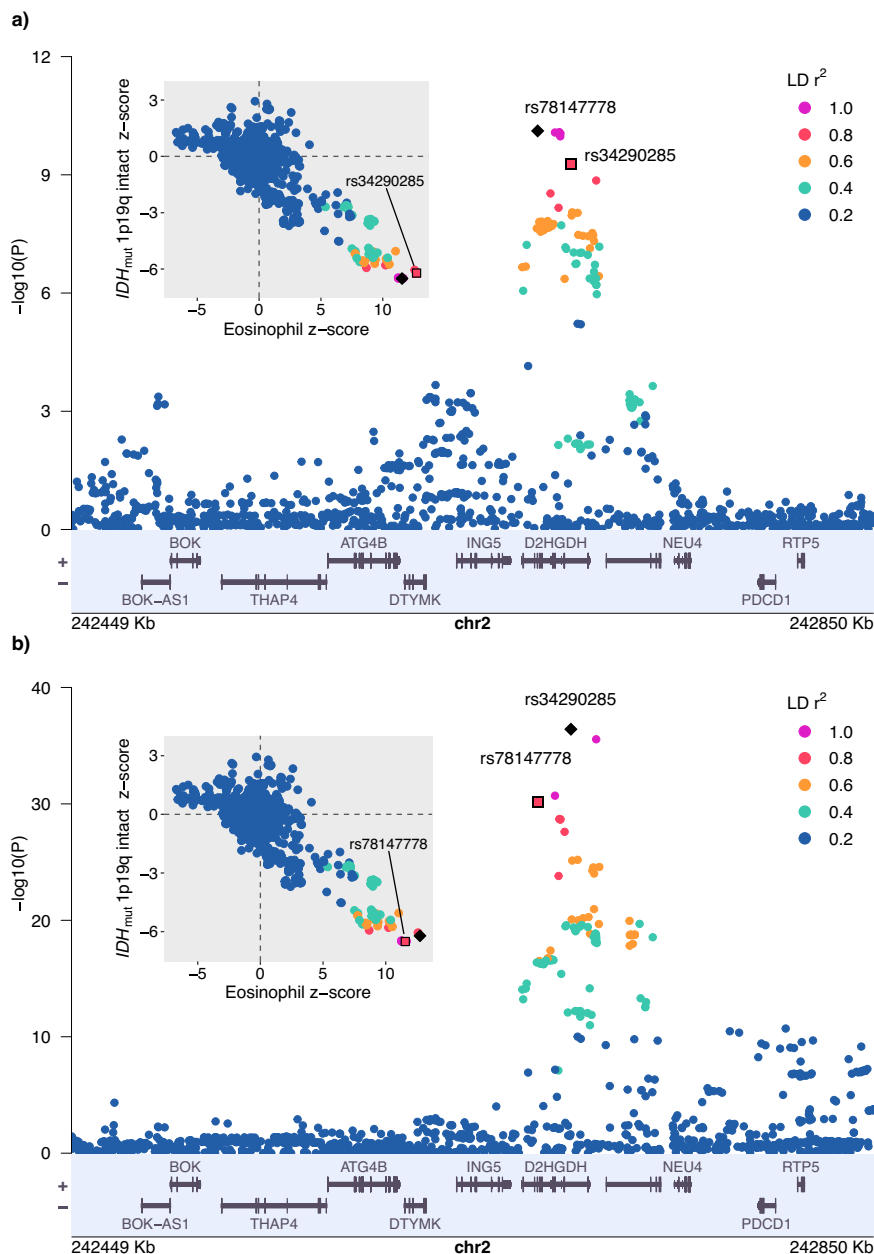
Fig. 4 | Colocalization of IDH mutated 1p/19q intact glioma risk locus in 2q37.3 eosinophil counts. Regional plots show two-sided GWAS *p*-values for (**a**) IDH$_{mut-}$$_{intact}$ glioma (615 cases, 8156 controls) based on logistic regression and (**b**) eosinophil counts (*n* = 234,763) based on linear regression. Inset panels show Wald test statistics (*z*-scores) for each phenotype. Linkage disequilibrium R^2 values are calculated with respect to the lead variant for each phenotype, denoted by the black diamond. The lead instrument for eosinophil counts, rs34290285, is also labeled.

cancer development and ensuing treatments. We observed that the effects of genetic regulators of blood cell homeostasis on glioma risk and survival were modified by IDH mutation and 1p/19q co-deletion status. Although we did not detect effects in opposite directions across molecular subtypes, most exposure-outcome relationships were subtype-specific, indicating germline differences in susceptibility to immune-mediated risk factors. This complements previously observed differences in genetic susceptibility loci for these molecular subtypes[3,37].

We found that genetic predisposition to higher circulating levels of lymphocytes and neutrophils were inversely associated with risk of IDH$_{mut}$ gliomas, particularly the IDH$_{mut}$ 1p/19q intact subtype. Colocalization of GWAS-identified glioma risk variants at 2q37.3 and 5p15.33 with blood cell traits also supports the existence of shared genetic mechanisms. The 2q37.3 (*D2HGDH*) risk locus for IDH$_{mut}$ was discovered in the UCSF and Mayo Clinic study[37] and the colocalized signal mapped to rs34290285, an instrument for eosinophils that has been linked to asthma and allergic diseases[38]. The protective effects observed for lymphocytes is broadly compatible with the hypothesis that this is a marker of improved immunosurveillance of cancer cells[39]. Genetic instruments in our study were developed in individuals without autoimmune or inflammatory conditions[22], suggesting that benign elevation of lymphocytes may confer some advantages, such as improved recognition of precursor lesions or more efficient elimination of early cancers[39–41].

Early versions of the immunosurveillance model attributed protective tumor immunity to antigen-specific lymphocytes, and it is now recognized that CD8+ and CD4+ T-cell responses play a critical role in immune clearance of tumor cells[39,40]. Our genetic instruments lacked resolution at the cell-type level to investigate this directly, but our
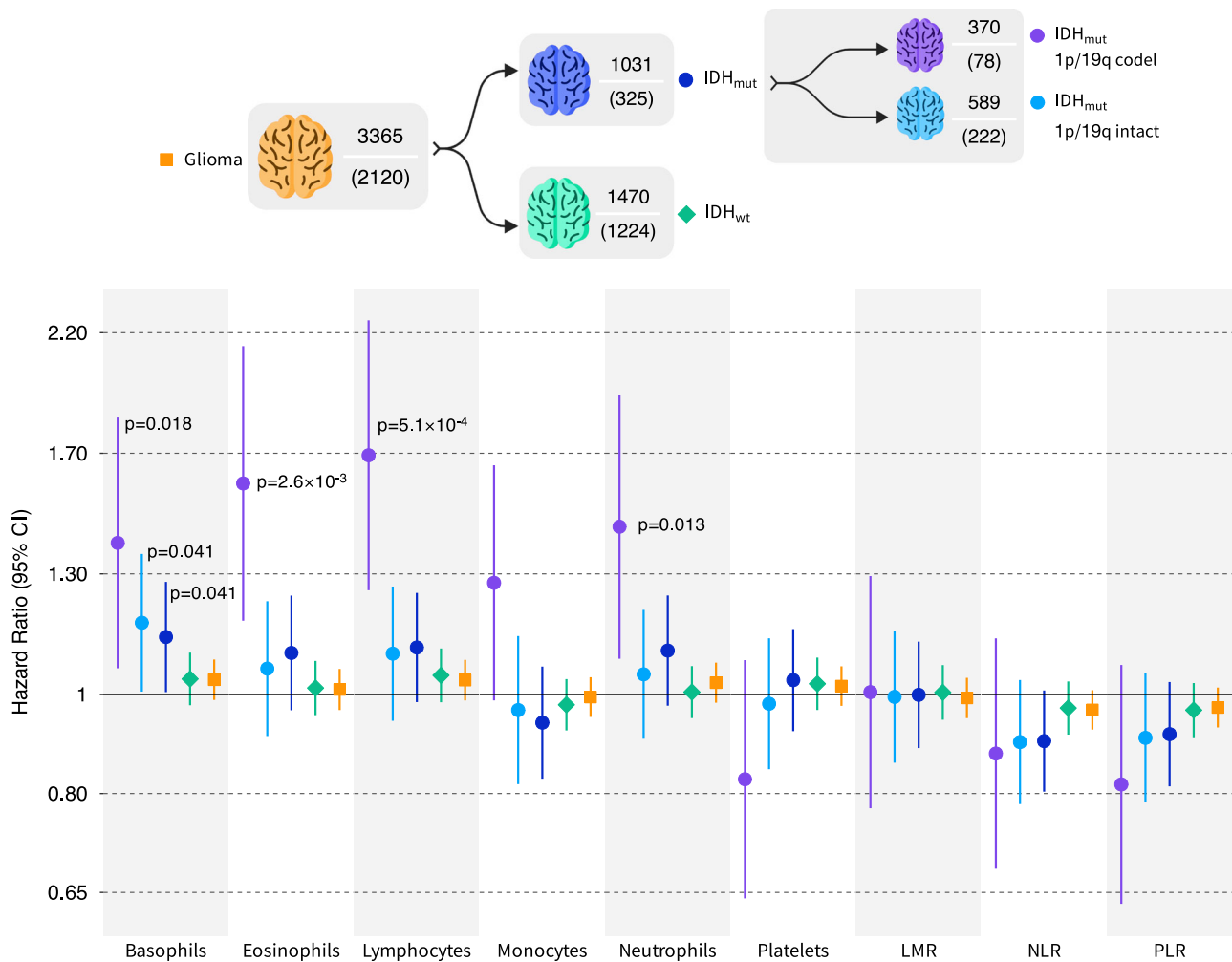
Fig. 5 | Meta-analysis of blood cell trait polygenic scores (PGS) associations with survival. Visualization of hazard ratios (HR) and 95% confidence intervals (CI) corresponding to the effect of a standard deviation increase in the standardized PGS on all-cause mortality. Two-sided *p*-values based on Cox proportional hazards models are reported for statistically significant associations. The sample size and corresponding number of mortality events is reported for each glioma subgroup.

findings for lymphocytes are aligned with Ostrom et al.[17], who reported a negative genetic correlation for lymphocyte percentage and risk of non-glioblastoma tumors, which are characterized by a high prevalence of IDH mutations. This study also detected negative genetic correlations with several autoimmune conditions and heritability enrichments among T cells, NK cells, and myeloid cells[17], suggesting that immune activation modifies the risk of glioma.

In contrast to lymphocytes, persistent neutrophil activation and infiltration is a hallmark of chronic inflammation associated with immunosuppression, tumor progression, and poor survival[42]. Neutrophils are the most abundant immune cell type. They are the first line of defense against invading pathogens and act as a bridge between innate and adaptive immune response[42]. Neutrophils are ascribed different roles in cancer depending on disease stage and can transition from exerting antitumor effects, such as CD8+ and CD4+ T cell priming, to cancer-promoting effects[42–44]. Circulating neutrophils are comprised of diverse cell populations displaying phenotypic heterogeneity and plasticity[42,45]. In addition to classic antitumorigenic and pro-tumorigenic neutrophils, there is a distinction between high-density neutrophils (HDNs), characterized by an immunostimulatory profile, and low-density neutrophils (LDNs) that consist of immature myeloid-derived suppressor cells with an immunosuppressive phenotype[42,45]. Peripheral blood in healthy individuals predominantly consists of HDNs, while LDNs accumulate during chronic inflammation

and malignancy[42,45]. Transforming growth factor β (TGF-β) can induce a transition from the HDN to the LDN phenotype, which is accompanied by loss of cytotoxic properties and gain of CD8+ T-cell suppression[42,45]. Although our genetic instruments do not distinguish neutrophil classes, the risk reducing effects observed for *IDH* mutated tumors may reflect tumor suppressive properties of healthy neutrophil populations. This is also supported by in-vitro evidence that human polymorphonuclear neutrophils display innate abilities to target and destroy cancer cells[46].

Our MR analysis uncovered that genetic propensity towards increased PLR, which indicates a higher relative abundance of platelets to lymphocytes, conferred an increased risk of IDH_mut glioma. The largest magnitude of effect observed for IDH_mut 1p/19q intact tumors. Although there was an attenuated, nominally significant PLR association for all gliomas combined, MR estimates for IDH_wt became reversed in sensitivity analyses, suggesting that the impact of PLR on disease susceptibility is likely restricted to the IDH_mut subtype. Platelets patrol the circulatory system and become activated in response to vessel damage and bacterial infection. Wound-healing and proangiogenic properties of platelets, including stimulation of vascular endothelial growth factor (VEGF) and fibroblast growth factor, have been proposed as a plausible mechanism by which elevated platelet counts may predispose to tumor development[47,48]. However, platelet elevation alone was not associated with increased disease risk, suggesting
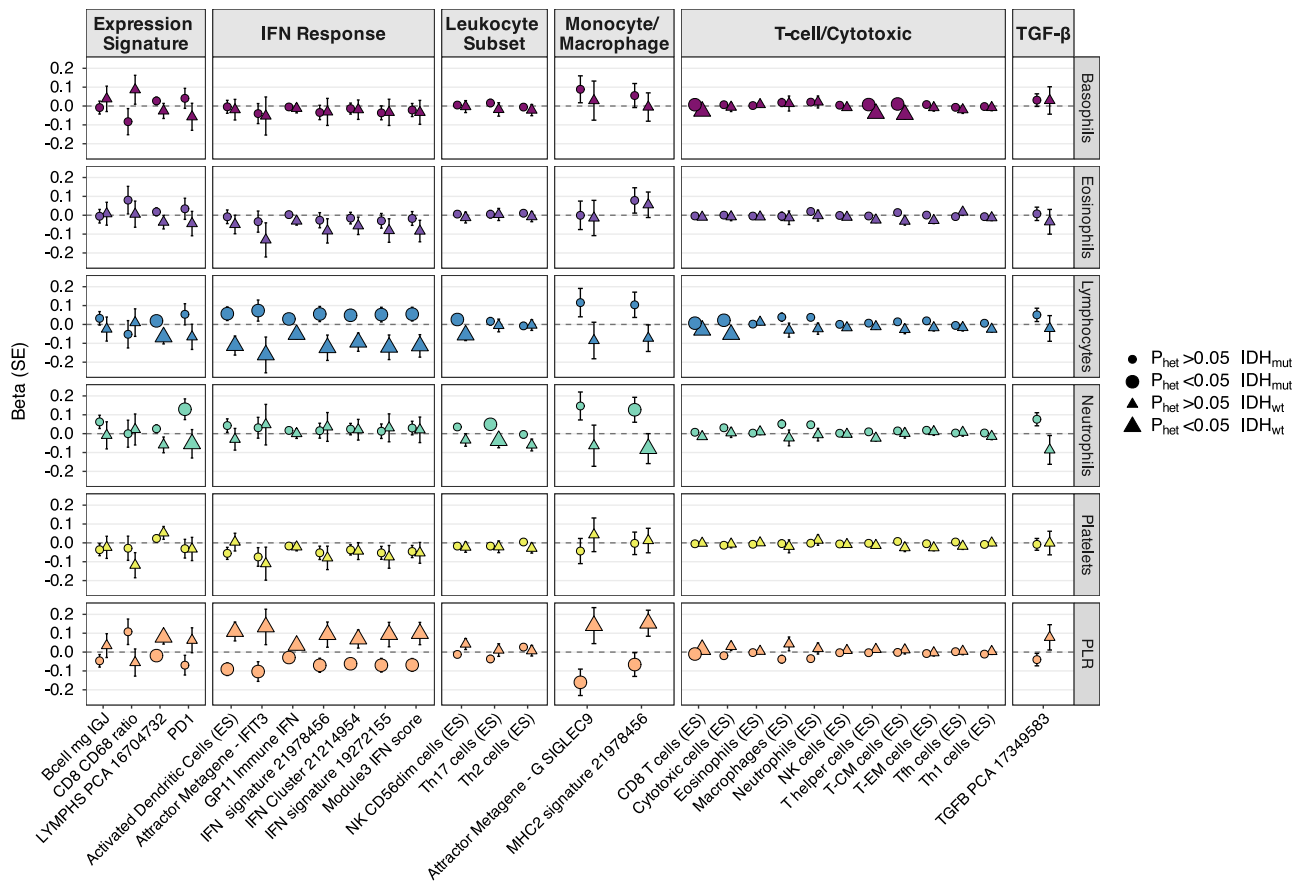
Fig. 6 | Associations of blood cell trait polygenic scores (PGS) with tumor immune microenvironment (TIME) features in TCGA. Associations for selected blood cell trait PGS with heritable TIME features identified in TCGA by Sayaman et al. (2021)[36]. Heterogeneity in PGS effect on specific TIME features between IDH mutant ($n = 369$) and IDH wildtype ($n = 364$) tumors was tested using Cochran's Q test (P_{het}). Data are presented as linear regression coefficients $+/-$ standard errors (SE). For enrichment score (ES) phenotypes beta coefficients were estimated per 10-unit change. All p-values are two-sided.

that the mechanisms underlying the PLR association likely involve dysregulation of platelet interaction with lymphocytes.

Immune-sensing platelets participate in innate and adaptive responses, coordinate pro-inflammatory signaling, providing multiple candidate mechanisms through which platelets may contribute to carcinogenesis[47]. Platelets interact with lymphocytes through direct cell-to-cell contact and soluble signaling. Outside of the context of infection, interactions of platelets with immune cells have been shown to be involved in atherosclerosis and inflammation[49], and emerging evidence suggests that platelets may dampen lymphocyte effector functions in the tumor microenvironment[48]. Platelets contain high levels of nonsignaling TGF-β and are the only cell population to constitutively express its docking receptor, glycoprotein A repetitions predominant (GARP), required for TGF-β activation[50,51]. In a murine model, TGF-β activated by platelet-expressed GARP suppressed T cell function and adoptive T cell therapy[51]. However, the interplay between systemic factors proxied by our genetic instruments and local immune response in the tumor is not well characterized[41].

Our MR analysis did not implicate genetic regulation of blood cell traits as a risk factor for IDH_wt tumors. However, there was evidence of colocalization with IDH_wt susceptibility in 5p15.33 and genetic regulation of neutrophils, platelets, PLR, and telomere length. This is consistent with previous work showing multiple candidate mechanisms in this highly pleiotropic locus, not limited to telomere maintenance[52]. Genetic signals for blood cell traits did not colocalize in 8q24, consistent with recent work demonstrating that rs55705857, the causal risk variant at this locus, exerts its effects through interaction with the *Myc* promoter and increased *Myc* expression[53].

We identified statistically significant associations with blood cell trait PGS only in IDH_mut 1p/19q co-deleted tumors, which may partly reflect longer median survival in these patients and greater power to detect factors that modify survival trajectories. In contrast to disease susceptibility, genetic predisposition to higher circulating counts of basophils, eosinophils, lymphocytes, and neutrophils were associated with higher risk of early death. These findings suggest that inflammation and immunity have a double role, being protective in the immunosurveillance phase, while detrimental during tumor progression.

In advanced-stage cancer, neutrophils can adopt a potent immunosuppressive role, particularly when they transform into polymorphonuclear myeloid-derived suppressor cells (MDSCs), sharing characteristics with immature neutrophils. Emerging evidence suggests that even early neutrophil progenitors, MDSCs, may contribute to pro-tumor activity[45]. Neutrophils are a key mediator of immune suppression in glioma[54] and have been observed to increase with glioma progression[55]. Notably, the stage of the disease, the specific tumor type, and the tissue context collectively determine whether specific cell types promote or hinder cancer progression. We also note that opposing effects on disease risk and survival were not detected within the same tumor type – MR risk estimates for the effect of blood cell traits on IDH_mut 1p/19q co-deleted tumors were null. The impact of genetic predictors of blood cell traits on survival may interact with somatic mutations within the tumor resulting in differences in TIME. This is supported by heterogeneity in blood cell PGS associations with TME features in TCGA glioma cases, stratified by IDH mutation status.

Differences in the immune landscape of IDH_mut and IDH_wt tumors are well established and attributed to the accumulation of the D-2HG

oncometabolite produced by the mutant IDH enzyme, which results in widespread hypermethylation and gene repression[56]. In addition to downregulating immune-related signaling, D-2HG has been shown to directly suppress T cell activation and lower the expression MHC class II, CD80, and CD86 molecules, further reducing capacity for antigen presentation[56,57]. This aligns with our observations of significant heterogeneity in basophil, neutrophil, and lymphocyte PGS effects on MHC-II, CD8 T cell, and cytotoxic T cell TIME signatures.

The neutrophil PGS was nominally associated with programmed cell death protein-1 (PD-1) TIME signature in IDH$_{mut}$ tumors only and this PGS effect showed significant heterogeneity by IDH status. PD-1 and its ligand PD-L1 have been shown to delay neutrophil apoptosis[58], which may be related to our inverse risk association with neutrophils in IDH$_{mut}$ tumors. PD-1/PD-L1 check point inhibitors have been of interest as a potential glioma therapeutic, however most trials have focused on glioblastoma tumors (IDH$_{wt}$ according to WHO 2021) with limited success[59]. Our results suggest that the success of anti-PD-1/PD-L1 therapy may vary by IDH status and germline predisposition. Considering the impact of genetically driven changes in immune cell types on survival may inform the selection of patients into clinical trials.

We also observed differences in associations across interferon responses and PGS for lymphocytes between IDH$_{wt}$ and IDH$_{mut}$ tumors. Interferons such as IFN-γ can directly affect lymphocyte function, including cytotoxic CD8+ T-cells. Recent studies have highlighted the role of IFN-γ in glioblastoma, showing that reducing Notch-regulated IFN-γ signaling aids in the evasion of immune surveillance and reduces tumor clearance[60]. IDH$_{mut-codel}$ gliomas maintain the same immunologically cold phenotype as overall IDH$_{mut}$ gliomas, but little is known about specific effects of 1p/19q co-deletion on the TIME[61]. As IDH mutations alone are not sufficient for gliomagenesis[62], interactions with additional somatic events, potentially the 1p/19 co-deletion, may contribute to the observed results.

Taken together, our study builds on decades of research that has implicated aspects of immune function in the etiology of glioma. While findings of observational studies are vulnerable to reporting biases and reverse causation, genetic predictors are not affected by external factors that have disruptive effects on immune cell distributions, such as infections and treatment mediated effects. Our analysis benefits from the strength of the genetic instruments, which explain between 4.5% and 23.5% of target trait variation[22], and range of statistical approaches for evaluating the robustness of our conclusions to genetic confounding by pleiotropy. However, it will be important for future studies to undertake prospective validation of associations with risk and survival using pre-diagnostic blood samples. Mechanistic studies will also be required to elucidate relevant cell types with greater resolution and pinpoint the immune processes which they influence. While TCGA analyses highlight overlap between heritable components of the TIME and genetic regulation of blood cell counts, analyses of cell-specific expression in a larger cohort would help contextualize broader assumptions of enrichment. Future studies should also consider analyses of longitudinal samples to clarify how changes in specific immune cell populations at different time points may influence survival outcomes, and whether this is modified by modified by germline genetic profiles.

We refined our MR and survival results by molecular subtypes of glioma, which enhances its clinical relevance, but also reduces statistical power for some analyses. Future studies with larger sample sizes will be required to replicate these findings and consider additional tumor features, such as TERT and ATRX mutations. Our survival analyses also have several limitations, including incomplete information on clinical covariates, such as treatment. We were also unable to account for time-varying confounders, such as changes in BMI, medications, and health-related behaviors after disease onset. Our study was restricted to participants of European descent, which also limits

the generalizability of our findings. Lifetime risk of glioma varies by race/ethnicity in the US, with highest incidence rates observed in Non-Hispanic Whites and lowest in Black individuals[1]. The distribution of hematologic traits and their genetic architecture also varies significantly with ancestry, therefore future studies should prioritize recruitment of underrepresented patient populations. As the search for the causes of glioma and improved treatments of this highly complex and deadly cancer continues, interrogating the genetic architecture of disease susceptibility and progression will contribute valuable insights.

Methods
Study population
We assembled data from three case-control studies with available molecular and genetic data to facilitate analyses stratified by glioma subtypes, as described in Guerra et al.[16] Briefly, we analyzed 1973 cases from the Mayo Clinic and University of California San Francisco (UCSF) Adult Glioma Study (AGS) with 1859 controls from the Glioma International Case-Control Study (GICC), an additional 659 cases and 586 controls from the UCSF AGS, and 786 glioma cases from The Cancer Genome Atlas (TCGA) with 5711 controls from the Wellcome Trust Case Control Consortium (WTCCC)[3,37,63,64]. Imputation was performed using the TOPMed reference panel. Analyses were restricted to individuals of predominantly (>70%) European genetic ancestry with adjustment for age, sex, and top 10 genetic ancestry principal components. Sex-stratified analyses were not performed due to sample size limitations. Study-specific GWAS results were meta-analyzed for a total sample size of 3418 cases and 8156 controls (Supplementary Fig. 1). As our analyses are based on historic cohort data, we lack the full set of molecular markers required to align our case definitions with WHO 2021 glioma classifications. However, using the available information we delineated prognostically significant phenotypes that distinguished IDH mutated (IDH$_{mut}$), IDH mutated 1p/19q co-deleted (IDH$_{mut-codel}$), IDH mutated without 1p/19q co-deletion (IDH$_{mut-intact}$), and IDH wildtype (IDH$_{wt}$) tumors. Collection of patient samples and associated clinicopathological information was undertaken with written informed consent and ethical board approval was obtained from the UCSF Committee on Human Research (USA) and the Mayo Clinic Office for Human Research Protection (USA).

Mendelian randomization and colocalization
Mendelian randomization (MR) is a statistical method that can infer causal exposure-outcome relationships under a strict set of assumptions by using genetic variants strongly associated with the exposure. The basic MR framework involves fitting a weighted linear regression between effect sizes for the outcome and effect sizes for the exposure. If all instruments are valid, the resulting slope provides an estimate of the causal effect of the exposure. Genetic instruments for blood cell traits were developed in the UK Biobank (UKB) cohort, as described in Kachuri et al.[22], and applied to the glioma GWAS meta-analysis (3418 cases and 8156 controls). Briefly, blood samples obtained from UKB participants aged 40-69 years at enrollment in 2006–2010 and analyzed within 24 hours using Beckman Coulter LH750 instruments at the UKB central laboratory. We performed a two-stage GWAS in participants of predominantly European ancestry, splitting the dataset into discovery (70%) and replication (30%), was followed by Multi-Trait Analysis of GWAS (MTAG)[65]. Our GWAS excluded individuals who were ever diagnosed with cancer or other conditions that may alter blood cell profiles. Genetic instruments for blood cell traits were selected from MTAG results based on the following criteria: linkage disequilibrium (LD) $r^2 < 0.05$ with a 10 Mb window with discovery $P < 5 \times 10^{-8}$ and replication $P < 0.05$. All GWAS p-values are two-sided.

A fundamental, but untestable, MR assumption of "no horizontal pleiotropy" requires that instruments influence the outcome exclusively through the exposure of interest, without any direct effects on

risk. Since this assumption cannot be verified, the sensitivity of the observed results to different scenarios of pleiotropy were assessed by examining consistency across multiple MR estimators. Maximum likelihood (ML) is the most restrictive method, unbiased only when all instruments are valid. Inverse variance weighted multiplicative random-effects (IVW-MRE) accounts for heterogeneity caused by non-directional pleiotropy[66,67]. MR Egger was reported if directional horizontal pleiotropy was suggested by the deviation of the Egger intercept from 0 (two-sided $p < 0.10$). Weighted median (WM)[28] allows up to 50% of the weights to be contributed by invalid instruments. MR RAPS (Robust Adjusted Profile Score)[26,27] employs a robust loss function to limit the influence of outlier instruments. MR pleiotropy residual sum and outlier (PRESSO)[25] tests for heterogeneity and corrects for the difference between the observed residual sum of squares and the expectation, simulated under the null hypothesis of no horizontal pleiotropy. To account for instances where MR-PRESSO detects pleiotropy, but is unable to pinpoint specific outliers, we used MR Radial[30] to identify variants that drive the observed heterogeneity. The default implementation of MR Radial was used, with modified second order weights[68] and a nominal ($p < 0.05$) threshold for outlier detection, as opposed to the Bonferroni threshold ($p < 0.05/$number of instruments) used by MR-PRESSO. In all MR analyses, odds ratios (OR) and 95% confidence intervals (CI) correspond to a genetically predicted standard deviation (SD) increase in lymphocytes, monocytes, neutrophils, basophils, and eosinophils. For blood cell ratios, effects were estimated per one unit increase.

Given the correlated nature of blood cell traits, multivariable MR was performed to estimate conditional effects on glioma risk by simultaneously regressing all instruments across all exposures. In addition to inverse variance weighting (MV-IVW) we also performed regularization-based MVMR, where the penalty controlling level of sparsity is tuned based on heterogeneity (MV-LASSO)[69]. To reduce collinearity in the MV-LASSO model, which was applied to cell ratios and their component traits, we performed an additional round of clumping to ensure that the genetic instruments were independent across all exposures.

Colocalization with glioma risk loci
We fine-mapped associations at genetic loci for blood cell traits that also reached genome-wide significance ($P < 5 \times 10^{-8}$) in for at least one glioma subtype in our data using SuSiE (SUm of SIngle Effects)[32,33]. SuSiE-colocalization was performed in a 500-bp region centered on the risk variant to estimate the posterior probability of a shared causal signal for disease susceptibility and regulation of blood cell homeostasis (PP_{H4}). For genetic variants that were associated with multiple candidate mechanisms, we also used HyPrColoc[70], although this approach does not relax the assumption of a single causal variant.

Genetic associations with survival
We explored associations between genetically predicted blood cell profiles and survival in glioma patients by fitting a polygenic score (PGS) for each trait computed as a weighted sum of trait-increasing alleles:

$$PGS = \beta_1 \times SNP_1 + \beta_2 \times SNP_2 + \ldots + \beta_n \times SNP_n \qquad (1)$$

with weights (β) corresponding to the same effect sizes as those used in the MR analysis. Hazard ratios (HR) per SD increase in the standardized PGS were estimated using a Cox proportional hazards model with adjustment for age, sex, the top 10 principal components (PCs) of genetic ancestry, and study site for the combined UCSF AGS and Mayo Clinic case series. We also performed sensitivity analyses adjusting for additional clinical covariates, such as disease grade and type of treatment. Follow-up time was calculated from the date of first surgery to

either date of death or date of last known contact. Study-specific PGS associations were meta-analyzed.

Significant PGS associations were followed up in Mendelian randomization analyses, however, assessing causality for disease progression endpoints is complicated by index event bias[71,72]. Selection based on disease status in case-only analyses may introduce bias into genetic associations with progression because cancer risk factors may become correlated when restricting to cases, which in turn may induce associations between risk factors and cancer progression events[72]. We applied the Dudbridge et al.[72] method to 41,528 pruned variants (LD $r^2 < 0.10$ in 250 kb windows) with MAF ≥ 0.05 and INFO > 0.90 to test for the presence of index event bias and estimate the corresponding correction factor (b). This approach regresses SNP effects on risk against their effects on survival[72]. Bias-corrected effects on survival are estimated as follows:

$$\beta'_{surv} = \beta_{surv} - b * \beta_{risk} \qquad (2)$$

where β_{risk} is obtained from the case-control glioma GWAS.

Genetic associations with the tumor immune microenvironment (TIME) features
We examined associations between selected blood cell trait PGS and heritable tumor immune microenvironment features identified by Sayaman et al.[36] in TCGA. Linear regression models for each TIME feature were fit separately IDH_{mut} and IDH_{wt} cases and adjusted for age, sex, and the top 10 genetic ancestry PCs. Of the 33 pan-cancer immune phenotypes, 28 were available for analysis in glioma subjects.

Reporting summary
Further information on research design is available in the Nature Portfolio Reporting Summary linked to this article.

Data availability
The raw genotype and phenotype data are protected and are not available due to data privacy laws, but can be obtained from the following repositories. Genotype data of control samples from the 1958 British Birth Cohort and UK Blood Service Control Group are available from the Wellcome Trust Case Control Consortium (WTCCC) and the European Genotype Archive under accession numbers EGAD00000000021 and EGAD00000000023. Genotype data of glioma cases from The Cancer Genome Atlas (TCGA) were obtained from Database of Genotypes and Phenotypes (dbGaP) under accession number phs000178 [https://www.ncbi.nlm.nih.gov/projects/gap/cgi-bin/study.cgi?study_id=phs000178.v11.p8]. Genotype data of control samples from the Glioma International Case Control Study (GICC) are available from dbGaP under accession number phs001319 [https://www.ncbi.nlm.nih.gov/projects/gap/cgi-bin/study.cgi?study_id=phs001319.v1.p1]. Genotype data for the UCSF Adult Glioma study is available from dbGaP under accession number phs001497 [https://www.ncbi.nlm.nih.gov/projects/gap/cgi-bin/study.cgi?study_id=phs001497.v2.p1]. Summary statistics for genetic instruments for blood cell traits are available in Zenodo https://doi.org/10.5281/zenodo.13761088. Source data are provided as a Source Data File and in Supplementary Tables. Source data are provided with this paper.

Code availability
Statistical analyses were performed using R (version 4.3.3). Mendelian Randomization analyses were performed using the TwoSampleMR (version 0.6.6) R package available from: https://github.com/MRCIEU/TwoSampleMR. Colocalization analyses were performed using the following R packages: coloc (version 5.2.3) https://cran.r-project.org/web/packages/coloc/index.html and HyPrColoc (version

1.0) https://github.com/jrs95/hyprcoloc. Figure 4 was created using the plotgardener (version 1.8.3) R package available from: https://github.com/PhanstielLab/plotgardener.

References

1. Ostrom, Q. T. et al. CBTRUS Statistical Report: Primary brain and other central nervous system tumors diagnosed in the United States in 2016–2020. *Neuro Oncol.* **25**, iv1–iv99 (2023).
2. Miller, K. D. et al. Brain and other central nervous system tumor statistics, 2021. *CA Cancer J. Clin.* **71**, 381–406 (2021).
3. Eckel-Passow, J. E. et al. Glioma Groups Based on 1p/19q, IDH, and TERT Promoter Mutations in Tumors. *N. Engl. J. Med.* **372**, 2499–2508 (2015).
4. Molinaro, A. M., Taylor, J. W., Wiencke, J. K. & Wrensch, M. R. Genetic and molecular epidemiology of adult diffuse glioma. *Nat. Rev. Neurol.* **15**, 405–417 (2019).
5. Molinaro, A. M. et al. Interactions of age and blood immune factors and non-invasive prediction of glioma survival. *J. Natl Cancer Inst.* **114**, 446–457 (2022).
6. Amirian, E. S. et al. History of chickenpox in glioma risk: a report from the glioma international case-control study (GICC). *Cancer Med.* **5**, 1352–1358 (2016).
7. Wrensch, M. et al. History of chickenpox and shingles and prevalence of antibodies to varicella-zoster virus and three other herpesviruses among adults with glioma and controls. *Am. J. Epidemiol.* **161**, 929–938 (2005).
8. Guerra, G. et al. Antibodies to varicella-zoster virus and three other herpesviruses and survival in adults with glioma. *Neuro Oncol.* **25**, 1047–1057 (2023).
9. Wiemels, J. L. et al. History of allergies among adults with glioma and controls. *Int J. Cancer* **98**, 609–615 (2002).
10. Linos, E., Raine, T., Alonso, A. & Michaud, D. Atopy and risk of brain tumors: a meta-analysis. *J. Natl Cancer Inst.* **99**, 1544–1550 (2007).
11. Il'yasova, D. et al. Association between glioma and history of allergies, asthma, and eczema: a case-control study with three groups of controls. *Cancer Epidemiol. Biomark. Prev.* **18**, 1232–1238 (2009).
12. Amirian, E. S. et al. Approaching a scientific consensus on the association between allergies and glioma risk: a report from the glioma international case-control study. *Cancer Epidemiol. Biomark. Prev.* **25**, 282–290 (2016).
13. Wiemels, J. L. et al. Reduced immunoglobulin E and allergy among adults with glioma compared with controls. *Cancer Res.* **64**, 8468–8473 (2004).
14. Schwartzbaum, J. et al. Association between prediagnostic IgE levels and risk of glioma. *J. Natl Cancer Inst.* **104**, 1251–1259 (2012).
15. Disney-Hogg, L. et al. Impact of atopy on risk of glioma: a Mendelian randomisation study. *BMC Med.* **16**, 42 (2018).
16. Guerra, G. et al. The immunogenetics of viral antigen response is associated with sub-type specific glioma risk and survival. *Am. J. Hum. Genet.* **109**, 1105–1116 (2022).
17. Ostrom, Q. T. et al. Partitioned glioma heritability shows subtype-specific enrichment in immune cells. *Neuro Oncol.* **23**, 1304–1314 (2021).
18. Nduom, E. K., Weller, M. & Heimberger, A. B. Immunosuppressive mechanisms in glioblastoma. *Neuro Oncol.* **17**, vii9–vii14 (2015).
19. Grabowski, M. M. et al. Immune suppression in gliomas. *J. Neurooncol.* **151**, 3–12 (2021).
20. Bracci, P. M. et al. Pre-surgery immune profiles of adult glioma patients. *J. Neurooncol.* **159**, 103–115 (2022).
21. Wiencke, J. K. et al. Immunomethylomic approach to explore the blood neutrophil lymphocyte ratio (NLR) in glioma survival. *Clin. Epigenet.* **9**, 10 (2017).
22. Kachuri, L. et al. Genetic determinants of blood-cell traits influence susceptibility to childhood acute lymphoblastic leukemia. *Am. J. Hum. Genet.* **108**, 1823–1835 (2021).
23. Astle, W. J. et al. The allelic landscape of human blood cell trait variation and links to common complex disease. *Cell* **167**, 1415–1429.e1419 (2016).
24. Vuckovic, D. et al. The polygenic and monogenic basis of blood traits and diseases. *Cell* **182**, 1214–1231.e1211 (2020).
25. Verbanck, M., Chen, C. Y., Neale, B. & Do, R. Detection of widespread horizontal pleiotropy in causal relationships inferred from Mendelian randomization between complex traits and diseases. *Nat. Genet.* **50**, 693–698 (2018).
26. Zhao, Q., Chen, Y., Wang, J. & Small, D. S. Powerful three-sample genome-wide design and robust statistical inference in summary-data Mendelian randomization. *Int. J. Epidemiol.* **48**, 1478–1492 (2019).
27. Zhao, Q., Wang, J., Hemani, G., Bowden, J. & Small, D. S. Statistical inference in two-sample summary-data Mendelian randomization using robust adjusted profile score. *Ann. Stat.* **48**, 1742–1769 (2020).
28. Bowden, J., Davey Smith, G., Haycock, P. C. & Burgess, S. Consistent estimation in Mendelian randomization with some invalid instruments using a weighted median estimator. *Genet Epidemiol.* **40**, 304–314 (2016).
29. Bowden, J. et al. Assessing the suitability of summary data for two-sample Mendelian randomization analyses using MR-Egger regression: the role of the I2 statistic. *Int J. Epidemiol.* **45**, 1961–1974 (2016).
30. Bowden, J. et al. Improving the visualization, interpretation and analysis of two-sample summary data Mendelian randomization via the Radial plot and Radial regression. *Int J. Epidemiol.* **47**, 1264–1278 (2018).
31. Hemani, G., Tilling, K. & Davey Smith, G. Orienting the causal relationship between imprecisely measured traits using GWAS summary data. *PLoS Genet.* **13**, e1007081 (2017).
32. Wallace, C. A more accurate method for colocalisation analysis allowing for multiple causal variants. *PLoS Genet.* **17**, e1009440 (2021).
33. Zou, Y., Carbonetto, P., Wang, G. & Stephens, M. Fine-mapping from summary data with the "Sum of Single Effects" model. *PLoS Genet.* **18**, e1010299 (2022).
34. Walsh, K. M. et al. Telomere maintenance and the etiology of adult glioma. *Neuro Oncol.* **17**, 1445–1452 (2015).
35. Saunders, C. N. et al. Relationship between genetically determined telomere length and glioma risk. *Neuro Oncol.* **24**, 171–181 (2022).
36. Sayaman, R. W. et al. Germline genetic contribution to the immune landscape of cancer. *Immunity* **54**, 367–386 e368 (2021).
37. Eckel-Passow, J. E. et al. Adult diffuse glioma GWAS by molecular subtype identifies variants in D2HGDH and FAM20C. *Neuro Oncol.* **22**, 1602–1613 (2020).
38. Zhu, Z. et al. A genome-wide cross-trait analysis from UK Biobank highlights the shared genetic architecture of asthma and allergic diseases. *Nat. Genet.* **50**, 857–864 (2018).
39. Dadi, S. et al. Cancer immunosurveillance by tissue-resident innate lymphoid cells and innate-like T cells. *Cell* **164**, 365–377 (2016).
40. Chow, M. T., Moller, A. & Smyth, M. J. Inflammation and immune surveillance in cancer. *Semin. Cancer Biol.* **22**, 23–32 (2012).
41. Hiam-Galvez, K. J., Allen, B. M. & Spitzer, M. H. Systemic immunity in cancer. *Nat. Rev. Cancer* **21**, 345–359 (2021).
42. Giese, M. A., Hind, L. E. & Huttenlocher, A. Neutrophil plasticity in the tumor microenvironment. *Blood* **133**, 2159–2167 (2019).
43. Eruslanov, E. B. et al. Tumor-associated neutrophils stimulate T cell responses in early-stage human lung cancer. *J. Clin. Invest.* **124**, 5466–5480 (2014).
44. Pylaeva, E. et al. During early stages of cancer, neutrophils initiate anti-tumor immune responses in tumor-draining lymph nodes. *Cell Rep.* **40**, 111171 (2022).

45. Sagiv, J. Y. et al. Phenotypic diversity and plasticity in circulating neutrophil subpopulations in cancer. *Cell Rep.* **10**, 562–573 (2015).

46. Yan, J. et al. Human polymorphonuclear neutrophils specifically recognize and kill cancerous cells. *Oncoimmunology* **3**, e950163 (2014).

47. Gaertner, F. & Massberg, S. Patrolling the vascular borders: platelets in immunity to infection and cancer. *Nat. Rev. Immunol.* **19**, 747–760 (2019).

48. Haemmerle, M., Stone, R. L., Menter, D. G., Afshar-Kharghan, V. & Sood, A. K. The platelet lifeline to cancer: challenges and opportunities. *Cancer Cell* **33**, 965–983 (2018).

49. Huilcaman, R. et al. Platelets, a key cell in inflammation and atherosclerosis progression. *Cells* **11**, 1014 (2022).

50. Tran, D. Q. et al. GARP (LRRC32) is essential for the surface expression of latent TGF-beta on platelets and activated FOXP3+ regulatory T cells. *Proc. Natl Acad. Sci. USA* **106**, 13445–13450 (2009).

51. Rachidi, S. et al. Platelets subvert T cell immunity against cancer via GARP-TGFβ axis. *Sci. Immunol.* **2**, eaai7911 (2017).

52. Kachuri, L. et al. Mendelian Randomization and mediation analysis of leukocyte telomere length and risk of lung and head and neck cancers. *Int. J. Epidemiol.* **48**, 751–766 (2019).

53. Yanchus, C. et al. A noncoding single-nucleotide polymorphism at 8q24 drives IDH1-mutant glioma formation. *Science* **378**, 68–78 (2022).

54. Mi, Y. et al. The emerging role of myeloid-derived suppressor cells in the glioma immune suppressive microenvironment. *Front. Immunol.* **11**, 737 (2020).

55. Bayik, D. et al. Myeloid-derived suppressor cell subsets drive glioblastoma growth in a sex-specific manner. *Cancer Discov.* **10**, 1210–1225 (2020).

56. Richardson, L. G. et al. Implications of IDH mutations on immunotherapeutic strategies for malignant glioma. *Neurosurg. Focus* **52**, E6 (2022).

57. Bunse, L. et al. Suppression of antitumor T cell immunity by the oncometabolite (R)-2-hydroxyglutarate. *Nat. Med.* **24**, 1192–1203 (2018).

58. Wang, J. F. et al. Upregulated PD-L1 delays human neutrophil apoptosis and promotes lung injury in an experimental mouse model of sepsis. *Blood* **138**, 806–810 (2021).

59. Arrieta, V. A. et al. Immune checkpoint blockade in glioblastoma: from tumor heterogeneity to personalized treatment. *J. Clin. Invest.* **133**, e163447 (2023).

60. Parmigiani, E. et al. Interferon-gamma resistance and immune evasion in glioma develop via Notch-regulated co-evolution of malignant and immune cells. *Dev. Cell* **57**, 1847–1865.e1849 (2022).

61. Lin, B. D. et al. 2SNP heritability and effects of genetic variants for neutrophil-to-lymphocyte and platelet-to-lymphocyte ratio. *J. Hum. Genet.* **62**, 979–988 (2017).

62. Suzuki, H. et al. Mutational landscape and clonal architecture in grade II and III gliomas. *Nat. Genet.* **47**, 458–468 (2015).

63. Melin, B. S. et al. Genome-wide association study of glioma subtypes identifies specific differences in genetic susceptibility to glioblastoma and non-glioblastoma tumors. *Nat. Genet.* **49**, 789–794 (2017).

64. Wrensch, M. et al. Variants in the CDKN2B and RTEL1 regions are associated with high-grade glioma susceptibility. *Nat. Genet.* **41**, 905–908 (2009).

65. Turley, P. et al. Multi-trait analysis of genome-wide association summary statistics using MTAG. *Nat. Genet.* **50**, 229–237 (2018).

66. Burgess, S., Butterworth, A. & Thompson, S. G. Mendelian randomization analysis with multiple genetic variants using summarized data. *Genet. Epidemiol.* **37**, 658–665 (2013).

67. Bowden, J. et al. A framework for the investigation of pleiotropy in two-sample summary data Mendelian randomization. *Stat. Med.* **36**, 1783–1802 (2017).

68. Bowden, J. et al. Improving the accuracy of two-sample summary-data Mendelian randomization: moving beyond the NOME assumption. *Int J. Epidemiol.* **48**, 728–742 (2019).

69. Grant, A. J. & Burgess, S. Pleiotropy robust methods for multivariable Mendelian randomization. *Stat. Med.* **40**, 5813–5830 (2021).

70. Foley, C. N. et al. A fast and efficient colocalization algorithm for identifying shared genetic risk factors across multiple traits. *Nat. Commun.* **12**, 764 (2021).

71. Paternoster, L., Tilling, K. & Davey Smith, G. Genetic epidemiology and Mendelian randomization for informing disease therapeutics: Conceptual and methodological challenges. *PLoS Genet.* **13**, e1006944 (2017).

72. Dudbridge, F. et al. Adjustment for index event bias in genome-wide association studies of subsequent events. *Nat. Commun.* **10**, 1561 (2019).

Acknowledgements

Author contributions

All authors have given approval to the final version of the manuscript. Study was conceptualized by L.K. and S.S.F. Study design and primary data collection at UCSF was led by M.W. and J.K.W., with assistance from H.M.H., L.M., T.R., and A.M.M. Study design and data collection at the Mayo Clinic was led by R.B.J. and J.E.P. L.K. performed the Mendelian Randomization analyses, survival analyses, and polygenic score association analyses. TN performed colocalization analyses. G.A.G. and G.A.W. performed quality control, genotype imputation, and generated genome-wide association summary statistics. L.K. wrote the manuscript with discussions with S.S.F. All authors

contributed to the interpretation of results, reviewed, and edited the manuscript.

Competing interests

The authors declare no competing interests.

Additional information